Scientific
Research

Analysis of the Low-Energy $\pi^\pm p$ Elastic-Scattering Data

E. Matsinos[1*], G. Rasche[2]

[1]Centre for Applied Mathematics and Physics, Zurich University of Applied Sciences, Winterthur, Switzerland
[2]Institut für Theoretische Physik der Universität, Zürich, Switzerland
Email: *evangelos.matsinos@zhaw.ch

ABSTRACT

We report the results of a phase-shift analysis (PSA) of the low-energy $\pi^\pm p$ elastic-scattering data. Following the method which we had set forth in our previous PSA [1], we first investigate the self-consistency of the low-energy $\pi^\pm p$ elastic-scattering databases, via two separate analyses of (first) the $\pi^+ p$ and (subsequently) the $\pi^- p$ elastic-scattering data. There are two main differences to our previous PSA: 1) we now perform only *one* test for the acceptance of each data set (based on its contribution to the overall χ^2) and 2) we adopt a more stringent acceptance criterion in the statistical tests. We show that it is possible to obtain self-consistent databases after removing a very small amount of the data (4.57% of the initial database). We subsequently fit the ETH model [38] to the truncated $\pi^\pm p$ elastic-scattering databases. The model-parameter values show reasonable stability when subjected to different criteria for the rejection of single data points and entire data sets. Our result for the pseudovector πNN coupling constant is 0.0726 ± 0.0014. We extract the scattering lengths and volumes, as well as the *s*- and *p*-wave hadronic phase shifts up to $T = 100$ MeV. Large differences in the *s*-wave part of the interaction can be seen when comparing our hadronic phase shifts with the current SAID solution (WI08); there is general agreement in the *p* waves, save for the $\tilde{\delta}_{1-}^{1/2}$ hadronic phase shift.

Keywords: πN Elastic Scattering; πN Hadronic Phase Shifts; πN Coupling Constants; πN Threshold Constants

1. Introduction

This is the first of three papers dealing with issues of the pion-nucleon (πN) interaction at low energies (pion laboratory kinetic energy $T \leq 100$ MeV). The goal in this study is to update part of the material given in our previous phase-shift analysis (PSA) [1]. Hereafter, we will refer to that solution as UZH06, and to the one obtained in the present work as ZUAS12. We will show that the differences between these two solutions are small. In the second of the papers [2], we will address the self-consistency of the only $\pi^\pm p$ elastic-scattering data which appeared in the meantime, *i.e.*, of the measurements of Ref. [3], give details on the problems we encountered in the analysis of these measurements, and provide evidence to support our decision to retain the UZH06 initial $\pi^\pm p$ elastic-scattering databases. In the third paper [4], we will analyse all available experimental data for the

charge-exchange (CX) reaction $\pi^- p \to \pi^0 n$ and re-address the violation of the isospin invariance in the hadronic part of the πN interaction. In our program, we make use of the electromagnetic (em) corrections of Refs. [5], which lead to the em-modified hadronic quantities [1].

We re-open the case of the πN interaction at low energies because of three reasons.

- There have been changes in the values of the physical constants which we had used in order to obtain our UZH06 solution. The largest of these changes concern the values of the charge radii of the pion and of the proton. All physical constants will be fixed here to the recommended values of the most recent report of the Particle-Data Group [6].
- In view of the fact that a large amount of $\pi^\pm p$ elastic-scattering data became available in 2004, one might be under the impression that the important results and conclusions obtained with our UZH06 solu-

tion (which did not include these data) need to be revised; we will show that this is not the case. Due to numerous problems which we have encountered in the analysis of these data [2], we have decided not to include them in our database.

- A large amount of CX data appeared after the completion of the UZH06 PSA. In some cases, the corresponding reports of the experimental groups seem to cast doubt on the claims of isospin breaking [7,8]; therefore, it must be investigated whether the newly-obtained measurements invalidate those claims.

We must stress that the physical quantities appearing here (*i.e.*, the fit parameters of Sections 3.1-3.4, the scattering lengths and volumes of Section 3.4.2, the phase shifts of Section 3.4.3, etc.) are not purely-hadronic quantities since they still contain residual em effects, which the stage-I em corrections of Refs. [5] do not remove. These residual effects relate in particular to the fact that, in principle, the (unknown) hadronic masses should be used (in the hadronic part of the πN interaction) instead of the physical masses of the proton, of the neutron, and of the charged and neutral pion. Unfortunately, it is not possible at the present time to assess the significance of these effects. As a result, we must retain the cautious attitude of considering our physical quantities "em-modified hadronic" (as we did in Ref. [1]). However, the repetitive use of this term is clumsy. Therefore, we omit it, unless we consider its use necessary as, for instance, in Section 4 and in the captions of our tables and figures.

2. Method

2.1. Formalism

The determination of the observables from the hadronic phase shifts has been given in detail in Section 2 of Ref. [1]. For $\pi^+ p$ scattering, one obtains the partial-wave amplitudes from Equation (1) of that paper and determines the no-spin-flip and spin-flip amplitudes via Equations (2) and (3). Finally, the observables are evaluated from these amplitudes via Equations (13) and (14). For $\pi^- p$ elastic scattering, the observables are determined on the basis of Equations (15)-(20).

2.2. Minimisation Function and Scale Factors

Similarly to our previous PSA [1], we make use of the minimisation function given by the Arndt-Roper formula [9]. The contribution of the jth data set to the overall χ^2 is:

$$\chi_j^2 = \sum_{i=1}^{N_j} \left\{ \frac{z_j y_{ij}^{th} - y_{ij}^{\exp}}{\delta y_{ij}^{\exp}} \right\}^2 + \left(\frac{z_j - 1}{\delta z_j} \right)^2 \qquad (1)$$

where $y_{ij}^{\exp}$ denotes the ith data point of the jth data

set, y_{ij}^{th} the corresponding fitted value (also referred to as "theoretical"), $\delta y_{ij}^{\exp}$ the statistical uncertainty of the $y_{ij}^{\exp}$ data point, z_j a scale factor for the relative normalisation applying to the entire data set, δz_j the corresponding uncertainty (reported or assigned), and N_j the number of data points in the data set. The fitted values y_{ij}^{th} are obtained by means of parameterised forms of the *s*- and *p*-wave amplitudes. The values of the scale factor z_j are determined (for each data set separately) in such a way as to minimise χ_j^2. For each data set, there is a unique solution for z_j:

$$z_j = \frac{\sum_{i=1}^{N_j} y_{ij}^{th} y_{ij}^{\exp} \left/ \left(\delta y_{ij}^{\exp} \right)^2 + \left(\delta z_j \right)^{-2} \right.}{\sum_{i=1}^{N_j} \left(y_{ij}^{th} / \delta y_{ij}^{\exp} \right)^2 + \left(\delta z_j \right)^{-2}}, \qquad (2)$$

which leads to

$$\left(\chi_j^2 \right)_{\min} = \sum_{i=1}^{N_j} \frac{\left(y_{ij}^{th} - y_{ij}^{\exp} \right)^2}{\left(\delta y_{ij}^{\exp} \right)^2}$$
$$- \frac{\left\{ \sum_{i=1}^{N_j} y_{ij}^{th} \left(y_{ij}^{th} - y_{ij}^{\exp} \right) \left/ \left(\delta y_{ij}^{\exp} \right)^2 \right. \right\}^2}{\sum_{i=1}^{N_j} \left(y_{ij}^{th} / \delta y_{ij}^{\exp} \right)^2 + \left(\delta z_j \right)^{-2}} \qquad (3)$$

The overall $\chi^2 = \sum_{j=1}^{N} \left(\chi_j^2 \right)_{\min}$ (where N stands for the number of data sets used in the fit) is a function of the parameters entering the modelling of the *s*- and *p*-wave amplitudes; these parameters were varied until χ^2 attained its minimal value $\chi_{\min}^2$.

The part of $\left(\chi_j^2 \right)_{\min}$ which represents the pure random fluctuations in the measurements of the jth data set (*i.e.*, the "unexplained variation" in standard regression terminology) may be obtained from Equation (3) in the limit $\delta z_j \to \infty$, which is equivalent to removing the term $\left(\delta z_j \right)^{-2}$ from the denominator of the second term on the right-hand side (rhs) of the expression; we will denote this value by $\left(\chi_j^2 \right)_{st}$. The variation which is contained in $\left(\chi_j^2 \right)_{\min}$ in excess of $\left(\chi_j^2 \right)_{st}$ must be associated with the contribution from the rescaling (floating) of the data set as a whole; the expression for $\left(\chi_j^2 \right)_{sc} \equiv \left(\chi_j^2 \right)_{\min} - \left(\chi_j^2 \right)_{st}$ is

$$\left(\chi_j^2 \right)_{sc} = \frac{\left(\delta z_j \right)^{-2} \left\{ \sum_{i=1}^{N_j} y_{ij}^{th} \left(y_{ij}^{th} - y_{ij}^{\exp} \right) \left/ \left(\delta y_{ij}^{\exp} \right)^2 \right. \right\}^2}{\sum_{i=1}^{N_j} \left(y_{ij}^{th} / \delta y_{ij}^{\exp} \right)^2 \left\{ \sum_{i=1}^{N_j} \left(y_{ij}^{th} / \delta y_{ij}^{\exp} \right)^2 + \left(\delta z_j \right)^{-2} \right\}}. \qquad (4)$$

The scale factors which minimise only the first term on the rhs of Equation (1) are obtained from Equation (2) in the limit $\delta z_j \to \infty$:

$$\hat{z}_j = \frac{\sum_{i=1}^{N_j} y_{ij}^{th} y_{ij}^{exp} / \left(\delta y_{ij}^{exp}\right)^2}{\sum_{i=1}^{N_j} \left(y_{ij}^{th} / \delta y_{ij}^{exp}\right)^2}. \tag{5}$$

The scale factors of Equation (2) are appropriate when investigating the goodness of the overall reproduction of a data set in terms of a reference solution (yielding the fitted values). On the contrary, those of Equation (5) give maximal freedom to the baseline solution when determining the offset of a data set (with respect to that solution) and, as such, are more suitable when the emphasis is placed on the absolute normalisation, rather than on the overall reproduction, of a data set.

The statistical uncertainty in the evaluation of the scale factors $\hat{z}_j$ is given by

$$\delta \hat{z}_j = \frac{1}{\sqrt{\sum_{i=1}^{N_j} \left(y_{ij}^{th} / \delta y_{ij}^{exp}\right)^2}}. \tag{6}$$

When comparing the absolute normalisation of a data set with a reference solution, the statistical uncertainty of Equation (6) must be taken into account, along with the normalisation uncertainty $\delta \hat{z}_j$ of that data set. When investigating the absolute normalisation of some specific data sets, namely of those with suspicious absolute normalisation (e.g., see Section 3.4.6), the total uncertainty $\Delta \hat{z}_j = \sqrt{\delta \hat{z}_j^2 + \delta z_j^2}$ will be used.

2.3. Statistical Tests

For a data set containing N_j data points, $\left(N_j + 1\right)$ measurements have actually been made, the additional one relating to the absolute normalisation of the data set. Since the fit involves the fixing of each z_j at the value given in Equation (2), the proper number of degrees of freedom (hereafter, the acronym DOF will stand for "degree(s) of freedom", whereas NDF for the "number of DOF"), associated with the jth data set, is just N_j. This implies that the quantity $\left(\chi_j^2\right)_{min}$ of Equation (3) is expected to follow the χ^2 distribution with N_j DOF.

The essential difference between the present study and our previous PSA [1] is that only one statistical test for each data set will be performed here, the one involving its contribution $\left(\chi_j^2\right)_{min}$ to the overall χ^2; in Ref. [1], we instead performed tests for the shape and for the normalisation of each data set.

The p-value which is evaluated on the basis of $\left(\chi_j^2\right)_{min}$

and N_j will be compared with the confidence level p_{min} for the acceptance of the null hypothesis (no statistically-significant effects); in case that the extracted p-value is below p_{min}, the DOF with the largest contribution (to the $\left(\chi_j^2\right)_{min}$ value) will be eliminated in the subsequent fit. Only one point will be removed at each step, and the optimisation will be repeated. Data sets which do not give acceptable p-values (i.e., above p_{min}) after the elimination of two of their data points (the absolute normalisation is also considered to be one data point) will be removed from the database.

The second difference to Ref. [1], as far as the data analysis is concerned, relates to the choice of the confidence level which is assumed in the statistical tests; in Ref. [1], p_{min} was set to about 2.70×10^{-3} (which is equivalent to a 3σ effect in the normal distribution). Herein, we will instead adopt the p_{min} value which is associated with a 2.5σ effect; this value is approximately equal to 1.24×10^{-2}, that is, slightly larger than 1.00×10^{-2}, which is "commonly" (among statisticians) associated with the outset of statistical significance. In any case, only a few data (five DOF of the $\pi^\pm p$ elastic-scattering databases) are affected by this more stringent acceptance criterion.

3. Results

The repetitive use of the full description of the databases is largely facilitated if we adhere to the following notation: DB$_+$ for the $\pi^+ p$ database; DB$_-$ for the $\pi^- p$ elastic-scattering database; DB$_{+/-}$ for the combined $\pi^\pm p$ elastic-scattering databases.

The initial DB$_+$ comprises differential cross sections (DCSs) [10-18], analysing powers (APs) [19,20], partial-total cross sections (PTCSs) [21,22], and total (in fact total-nuclear) cross sections (TCSs) [23,24]. The initial DB$_+$ consists of 364 data points, distributed among 54 data sets, 26 of which relate to the DCS, 3 to the AP, and 25 (all one- or two-point data sets) to the PTCS and TCS. The initial DB$_-$ consists of 336 data points distributed among 36 data sets, i.e., 27 for the DCS ([12,13], [15-18], and [25]) and 9 for the AP ([19] and [26-28]).

We now list the measurements which have not been included in our analysis.

- The self-consistency of the $\pi^\pm p$ elastic-scattering DCS measurements of Ref. [3] will be addressed in detail elsewhere [2]. This is an enormous piece of experimental data, comparable in quantity to the database we established in our UZH06 PSA. Prior to their incorporation into a self-consistent set of data, the self-consistency of these measurements (as well as their compatibility with the established database) must be verified; in Ref. [2], we will come to a negative result.

- The 70 $\pi^+ p$ DCS measurements of Ref. [29] are obvious outliers in all exclusive analyses of the low-energy data; when using "traditional" statistics, the inclusion of these values in a PSA is bound to introduce spurious effects (e.g., drifting of the parameters during the optimisation, entrapment of the minimisation algorithms in local minima, failing fits, etc.). We will further comment on these data in Section 3.4.6.
- The 6 (3 for $\pi^+ p$ at 94.50 MeV, 3 for $\pi^- p$ at 88.50 MeV) DCS measurements of Ref. [30] have not appeared in a form which would enable their straightforward inclusion in our database. Furthermore, we are not convinced that the original DCS data may be retrieved by simply adding the contributions appearing in columns 4 and 5 of **Table 1** of Ref. [30].
- Given that the 9 existing $\pi^- p$ PTCSs and TCSs contain a component from CX scattering, they cannot be used; the inclusion of these data in any part of the analysis would perplex the discussion on the violation of the isospin invariance in the hadronic part of the πN interaction [4].
- The inclusion of the 28 AP measurements of Ref. [31] in the fits would necessitate substantial modifications in the database structure and in the analysis software. This is due to two reasons: 1) each of the three data sets, to which the measurements of Ref. [31] must be assigned, contains data taken at more than one beam energy and 2) the last of the data sets contains measurements for both elastic-scattering reactions. Given the difficulty at present to include these measurements in our fits, we can only use them in testing the overall consistency of our approach across energies. (If a significant amount of $\pi^- p$ measurements had been acquired in that experiment, we could have investigated the consistency of our approach across reactions.) We will return to this subject in Section 3.4.5.
- We will also not use in the fits the scattering length obtained from the experimental result for the strong shift of the 1s state in pionic hydrogen [32], after it has been corrected in Ref. [33] also taking into account the proper contributions of the γn channel; the difference to the $\tilde{a}^{cc}$ value of our UZH06 PSA (which is almost identical to the value we will obtain in this work) has been addressed in Ref. [33].

In order to give the data maximal freedom in the process of identifying the outliers, the two elastic-scattering reactions will be analysed separately using simple parameterisations of the s- and p-wave K-matrix elements. The (small at low energies) d and f waves have been fixed herein from the current SAID solution (WI08) [34]. In the SAID analysis, the energy dependence of the d and f phase shifts is determined from the region $T > 100$ MeV

(*i.e.*, from energies where these contributions are sizable). The largest of these phase shifts in the energy interval of this analysis, D15, does not exceed 0.27°.

For the purpose of fitting, the standard MINUIT package [35] of the CERN library was used (FORTRAN version). Each optimisation was achieved on the basis of the (robust) SIMPLEX-MINIMIZE-MIGRAD-MINOS chain. All fits of the present work terminated successfully.

3.1. Fits to the DB$_+$ Using the K-Matrix Parameterisations

The parameterisation, which we will now describe, was introduced (and successfully applied to $\pi^+ p$ scattering) in Ref. [36]. For $\pi^+ p$ elastic scattering, the s-wave phase shift is parameterised as

$$q_c \cot \tilde{\delta}_{0+}^{3/2} = \left(\tilde{a}_{0+}^{3/2} \right)^{-1} + b_3 \varepsilon + c_3 \varepsilon^2, \tag{7}$$

where q_c and ε are respectively the momentum and the pion kinetic energy in the centre-of-mass (CM) system. The $p_{1/2}$-wave phase shift is parameterised according to the form

$$\tan \tilde{\delta}_{1-}^{3/2} / q_c = d_{31} \varepsilon + e_{31} \varepsilon^2. \tag{8}$$

Since the $p_{3/2}$ wave contains the $\Delta(1232)$ resonance, a resonant piece in Breit-Wigner form is added to the background term, thus leading to the equation

$$\tan \tilde{\delta}_{1+}^{3/2} / q_c = d_{33} \varepsilon + e_{33} \varepsilon^2 + \frac{\Gamma_\Delta m_\Delta^2}{q_\Delta^3 W} \frac{q_c^2}{m_\Delta^2 - W^2}, \tag{9}$$

with $m_\Delta = 1232$ MeV and $\Gamma_\Delta = 118$ MeV [6]; q_Δ is the value of the CM momentum at the resonance position. The third term on the rhs of Equation (9) is the standard resonance contribution (e.g., see Ref. [37], p. 31).

The use of the parametric forms in Equations (7)-(9), which do not impose any theoretical constraints (save for the expected low-energy behaviour of the K-matrix elements and for the Breit-Wigner form used to describe the $\Delta(1232)$-resonance contribution), ensures that any outliers in the fits cannot be attributed to the inability of these forms to account for the energy dependence of the phase shifts; they are instead indicative of experimental problems.

Following the procedure of Section 2.3, we found that, for the data sets of BRACK90 [16] at 66.80 MeV and JORAM95 [18] at 32.70 MeV, the p-values were still below p_{min} after the removal of two data points (from each data set); as a result, these two data sets (with eleven and seven data points, respectively) were removed from the database. These two data sets have extremely low p-values and clearly stand out from the rest of the $\pi^+ p$ data. Two data sets had to be freely floated, the

Table 1. The data sets comprising the truncated $\pi^+ p$ database, the pion laboratory kinetic energy T (in MeV), the number of degrees of freedom $(NDF)_j$ for each data set, the scale factor z_j which minimises χ_j^2 of Equation (1), the values of $\left(\chi_j^2\right)_{min}$, and the p-value of the fit for each data set. The numbers of this table correspond to the final fit to the data using the K-matrix parameterisations (see Section 3.1).

Data set	T	$(NDF)_j$	z_j	$\left(\chi_j^2\right)_{min}$	p-value	Comments
AULD79	47.90	11	1.0146	15.6800	0.1534	
RITCHIE83	65.00	8	1.0434	17.2226	0.0279	
RITCHIE83	72.50	10	1.0047	4.7383	0.9080	
RITCHIE83	80.00	10	1.0289	19.0679	0.0394	
RITCHIE83	95.00	10	1.0327	13.1452	0.2157	
FRANK83	29.40	28	1.0161	19.4969	0.8821	
FRANK83	49.50	28	1.0458	33.4861	0.2183	
FRANK83	69.60	27	0.9282	23.6806	0.6480	
FRANK83	89.60	27	0.8614	29.2304	0.3498	
BRACK86	66.80	4	0.8901	2.4753	0.6491	freely floated
BRACK86	86.80	8	0.9380	15.9483	0.0431	freely floated
BRACK86	91.70	5	0.9736	11.6391	0.0401	
BRACK86	97.90	5	0.9723	7.2220	0.2046	
BRACK88	66.80	6	0.9458	11.5494	0.0728	
BRACK88	66.80	6	0.9554	10.1689	0.1177	
WIEDNER89	54.30	19	0.9871	14.7570	0.7379	
BRACK90	30.00	5	1.0830	10.6037	0.0598	79.40° removed
BRACK90	45.00	8	1.0124	7.6622	0.4671	
BRACK95	87.10	8	0.9730	13.8367	0.0861	
BRACK95	98.10	8	0.9810	14.8814	0.0615	
JORAM95	45.10	9	0.9600	20.1704	0.0169	124.42° removed
JORAM95	68.60	9	1.0506	8.2909	0.5051	
JORAM95	32.20	20	1.0138	33.5992	0.0290	
JORAM95	44.60	18	0.9528	29.9202	0.0382	30.74°, 35.40° removed
SEVIOR89	98.00	6	1.0157	5.4478	0.4878	
WIESER96	68.34	3	0.8899	2.6924	0.4415	
WIESER96	68.34	4	0.9202	3.8288	0.4297	
KRISS97	39.80	1	1.0129	1.9961	0.1577	
KRISS97	40.50	1	1.0019	0.1775	0.6735	
KRISS97	44.70	1	1.0027	0.0768	0.7817	
KRISS97	45.30	1	1.0034	0.0946	0.7584	
KRISS97	51.10	1	1.0246	3.5130	0.0609	
KRISS97	51.70	1	1.0029	0.0588	0.8084	
KRISS97	54.80	1	1.0077	0.1738	0.6768	
KRISS97	59.30	1	1.0256	1.2984	0.2545	
KRISS97	66.30	2	1.0497	4.0101	0.1347	
KRISS97	66.80	2	1.0074	0.5779	0.7491	

Continued

KRISS97	80.00	1	1.0136	0.3366	0.5618
KRISS97	89.30	1	1.0078	0.2795	0.5970
KRISS97	99.20	1	1.0560	4.2590	0.0390
FRIEDMAN99	45.00	1	1.0437	2.3178	0.1279
FRIEDMAN99	52.10	1	1.0182	0.2772	0.5986
FRIEDMAN99	63.10	1	1.0363	0.4904	0.4838
FRIEDMAN99	67.45	2	1.0517	1.2397	0.5380
FRIEDMAN99	71.50	2	1.0490	0.8114	0.6665
FRIEDMAN99	92.50	2	1.0429	0.5872	0.7456
CARTER71	71.60	1	1.0921	2.6734	0.1020
CARTER71	97.40	1	1.0498	0.6952	0.4044
PEDRONI78	72.50	1	1.0121	0.1329	0.7155
PEDRONI78	84.80	1	1.0311	0.3258	0.5682
PEDRONI78	95.10	1	1.0230	0.2030	0.6523
PEDRONI78	96.90	1	1.0167	0.1330	0.7153

BRACK86 [13] measurements at 66.80 and 86.80 MeV. Finally, four additional single data points were removed.

After the elimination of 24 DOF of the initial database, we obtain a truncated DB_+ comprising 52 data sets with 340 DOF. The surviving data sets and the corresponding NDF are listed in **Table 1**; the numbers have been taken from the final fit to the truncated DB_+ using the K-matrix parameterisations.

Since seven parameters were used in order to generate the fitted values, the NDF in the fit to the initial database was 357; the minimal value of χ^2 was 675.7. For the truncated database with 333 DOF in the fit, the minimal value of χ^2 was 427.2. Therefore, the elimination of only 24 DOF of the initial database leads to an impressive decrease of the χ^2 by 248.5 units. At the same time, the p-value of the fit increased by over 17 orders of magnitude.

3.2. Fits to the DB_- Using the K-Matrix Parameterisations

The $I = 3/2$ amplitudes, obtained in the final fit to the truncated DB_+ using the K-matrix parameterisations, were imported into the analysis of the DB_-. In this part, another seven parameters were introduced, to parameterise the $I = 1/2$ amplitudes. As in the $\pi^+ p$ case, these parameters were varied pursuing the minimisation of the χ^2 function. Similar parametric forms were used as those given in Equations (7)-(9), with the parameters $\tilde{a}_{0+}^{1/2}$, b_1, c_1, d_{13}, e_{13}, d_{11}, and e_{11}. Of course, there is no resonance term in the expression for $\tilde{\delta}_{1+}^{1/2}$; instead, it is necessary to include the contribution of the Roper

resonance in $\tilde{\delta}_{1-}^{1/2}$:

$$\tan \tilde{\delta}_{1-}^{1/2} / q_c = d_{11}\varepsilon + e_{11}\varepsilon^2 + \frac{\Gamma_N m_N^2}{q_N^3 W} \frac{q_c^2}{m_N^2 - W^2}, \quad (10)$$

with $m_N = 1440$ MeV and $\Gamma_N = 195$ MeV [6]; q_N denotes the CM momentum at the Roper-resonance position. As we are dealing with energies below the pion-production threshold, Γ_N is the elastic width.

The DB_- was also subjected to the tests described in Section 2.3. As in the UZH06 PSA, the BRACK90 [16] 66.80 MeV data set (containing five data points) was marked as an outlier. Two additional single data points had to be removed. Furthermore, the WIEDNER89 [15] data set had to be freely floated. After the elimination of 8 DOF of the initial DB_-, we obtain a truncated database comprising 35 data sets with 328 DOF (see **Table 2**). Since seven parameters were used in order to generate the fitted values, the NDF in the fit to the initial database was 329; the minimal value of χ^2 was 528.1. For the truncated database with 321 DOF in the fit, the minimal value of χ^2 was 371.0. At the same time, the p-value of the fit increased by 9 orders of magnitude.

3.3. Common Fit to the $DB_{+/-}$ Using the K-Matrix Parameterisations

Judged solely on the basis of the p-values, it appears that the truncated DB_+ and DB_- are not of the same quality. However, there is an appropriate statistical measure for such a comparison of two quantities following the χ^2 distribution. In order to prove that the two databases are of different quality (that is, that they have not been sam-

Table 2. The data sets comprising the truncated $\pi^- p$ elastic-scattering database, the pion laboratory kinetic energy T (in MeV), the number of degrees of freedom $(NDF)_j$ for each data set, the scale factor z_j which minimises χ_j^2 of Equation (1), the values of $\left(\chi_j^2\right)_{\min}$, and the p-value of the fit for each data set. The numbers of this table correspond to the final fit to the data using the K-matrix parameterisations (see Section 3.2).

Data set	T	$(NDF)_j$	z_j	$\left(\chi_j^2\right)_{\min}$	p-value	Comments
FRANK83	29.40	28	0.9832	30.9926	0.3174	
FRANK83	49.50	28	1.1007	30.1075	0.3581	
FRANK83	69.60	27	1.0953	25.6707	0.5369	
FRANK83	89.60	27	0.9479	25.4255	0.5506	
BRACK86	66.80	5	0.9973	13.9690	0.0158	
BRACK86	86.80	5	1.0036	1.4172	0.9224	
BRACK86	91.70	5	0.9963	2.8898	0.7170	
BRACK86	97.90	5	1.0002	5.9408	0.3120	
WIEDNER89	54.30	18	1.1597	23.6926	0.1654	15.55° removed, freely floated
BRACK90	30.00	5	1.0204	4.8808	0.4306	
BRACK90	45.00	9	1.0536	12.3031	0.1968	
BRACK95	87.50	6	0.9830	10.3543	0.1105	
BRACK95	98.10	7	1.0092	8.2223	0.3134	36.70° removed
JORAM95	32.70	4	0.9951	4.0883	0.3942	
JORAM95	32.70	2	0.9527	5.7974	0.0551	
JORAM95	45.10	4	0.9561	12.4590	0.0142	
JORAM95	45.10	3	0.9462	9.2581	0.0260	
JORAM95	68.60	7	1.0863	14.2673	0.0466	
JORAM95	68.60	3	1.0314	2.2747	0.5174	
JORAM95	32.20	20	1.0617	21.3392	0.3774	
JORAM95	44.60	20	0.9462	29.7408	0.0742	
JANOUSCH97	43.60	1	1.0420	0.1682	0.6817	
JANOUSCH97	50.30	1	1.0364	0.1557	0.6931	
JANOUSCH97	57.30	1	1.0830	4.5370	0.0332	
JANOUSCH97	64.50	1	0.9962	0.0010	0.9753	
JANOUSCH97	72.00	1	1.3045	4.8348	0.0279	
ALDER83	98.00	6	1.0335	5.0919	0.5321	
SEVIOR89	98.00	5	0.9882	1.5869	0.9028	
HOFMAN98	86.80	11	1.0020	5.8362	0.8841	
PATTERSON02	57.00	10	0.9365	11.0276	0.3554	
PATTERSON02	66.90	9	0.9985	4.3343	0.8881	
PATTERSON02	66.90	10	0.9479	18.0250	0.0545	
PATTERSON02	87.20	11	0.9835	8.2469	0.6910	
PATTERSON02	87.20	11	0.9945	5.0493	0.9288	
PATTERSON02	98.00	12	0.9954	6.9731	0.8594	

pled from the same distribution), the ratio

$$F = \frac{\chi_+^2 / NDF_+}{\chi_-^2 / NDF_-} \qquad (11)$$

must be significantly different from 1. In this formula, the subscripts "+" and "−" denote the two elastic-scattering reactions. The ratio F follows Fisher's (F) distribution. From the two final fits to the truncated databases using the K-matrix parameterisations, we obtain the score value of 1.110 for $NDF_+ = 333$ and $NDF_- = 321$ DOF in the two separate fits, which is translated into the p-value of 1.7×10^{-1}. Therefore, the claim about the dissimilarity of the two databases cannot be sustained. As a result, it makes sense to analyse the two reactions in terms of a common optimisation scheme.

In order to give the two elastic-scattering reactions equal weight, we multiplied $\left(\chi_j^2 \right)_{\min}$ for each $\pi^+ p$ data set by

$$w_+ = \frac{N_+ + N_-}{2N_+}$$

and for each $\pi^- p$ elastic-scattering data set by

$$w_- = \frac{N_+ + N_-}{2N_-},$$

where N_+ and N_- represent the NDF in the two databases; we then added these quantities for all the data sets to obtain the overall χ^2 value. The application of these "global" weights for the two reactions was made as a matter of principle; given that the values of N_+ and N_- are very close, the effect of this weighting on our results is very small.

The common fit to the truncated DB$_{+/-}$ (detailed in **Tables 1** and **2**) was made, using the 14 parameters of the K-matrix parameterisations given in Sections 3.1 and 3.2. We did not find any additional data points (or data sets) which had to be removed; we concluded that the truncated DB$_{+/-}$ are self-consistent. The common fit to the data yielded a χ^2 value of 792.4 for 654 DOF. The set of the excluded DOF represents 4.57% of the initial database. In the following, we will use this truncated DB$_{+/-}$.

3.4. Common Fits to the Truncated DB$_{+/-}$ Using the ETH Model

The modelling of the hadronic part of the πN interaction on the basis of the K-matrix parameterisations of Sections 3.1 and 3.2 is suitable as a first test of the self-consistency of the two elastic-scattering databases and as an efficient method for the identification of the outliers, yet neither does it provide insight into the underlying physical processes nor can it easily incorporate the important theoretical constraint of crossing symmetry.

In order to accomplish these two tasks, we will next involve in the analysis a model based on Feynman diagrams, namely the ETH model. This model was introduced in Ref. [38] and was developed further throughout the early 1990s. The ability of the ETH model to account for the low-energy $\pi^\pm p$ elastic-scattering data has been convincingly demonstrated over the past two decades.

The main diagrams on which this isospin-invariant model is based are graphs with scalar-isoscalar ($I = J = 0$) and vector-isovector ($I = J = 1$) t-channel exchanges, as well as the N and Δ s- and u-channel graphs. The main contributions to the partial-wave amplitudes from these diagrams have been given in detail in Ref. [38]. The small contributions from the six well-established four-star s and p higher baryon resonances with masses up to 2 GeV have also been analytically included in the model; in fact, the only significant contributions come from the Roper resonance. The tensor component of the $I = J = 0$ t-channel exchange was added in Ref. [8]; after this (insignificant) modification, no changes have been made to the model.

The $I = J = 0$ t-channel contribution to the amplitudes is approximated in the model by a broad $\pi\pi$ resonance, characterised by two parameters, G_σ and K_σ. Its exact position has practically no effect on the description of the πN scattering data or on the fitted values of G_σ and K_σ; for a long time, it has been fixed at 860 MeV. The $I = J = 1$ t-channel contribution is described by the ρ-meson, with $m_\rho = 775.49$ MeV [6]; this contribution introduces two additional parameters: G_ρ and K_ρ. The contributions of the s- and u-channel graphs with an intermediate N involve the πNN coupling constant $g_{\pi NN}$ and one additional parameter x representing the pseudoscalar admixture in the πNN vertex; for pure pseudovector coupling, $x = 0$. Finally, the contributions of the graphs with an intermediate Δ state introduce the coupling constant $g_{\pi N\Delta}$ and the parameter Z (which is associated with the spin-1/2 admixture in the Δ field). The higher baryon resonances do not introduce any parameters.

When a common fit of the ETH model to the data is made using all eight aforementioned parameters, it turns out that there is a strong correlation between G_σ, G_ρ, and x; due to this correlation, it is not possible to determine the values of all three quantities. We have chosen to set x to 0; this choice is usually adopted in effective-field theoretical models of low-energy πN scattering. The common fits of the ETH model to the truncated DB$_{+/-}$ will be performed on the basis of seven parameters: G_σ, K_σ, G_ρ, K_ρ, $g_{\pi NN}$, $g_{\pi N\Delta}$, and Z.

3.4.1. Model Parameters

The choice of the probability value below which data points must be excluded is difficult. We have adopted

here the value of p_{min} corresponding to a 2.5σ effect in the normal distribution. Recognising the subjectiveness in this choice, we consider that, in order to have confidence in the reliability of our analysis, it is necessary to verify that the fitted values of the seven model parameters remain stable over a reasonably broad range of p_{min} values; we followed the same strategy in Ref. [1]. Thus, in addition to $p_{min} \approx 1.24 \times 10^{-2}$, the analysis was performed with a database reduced by using the p_{min} values of about 2.70×10^{-3} (equivalent to a 3σ effect in the normal distribution) and 4.55×10^{-2} (equivalent to a 2σ effect in the normal distribution)[1].

Table 3 shows the values of the seven model parameters for the common fits to the truncated $DB_{+/-}$ for the three selected values of p_{min}. The uncertainties shown correspond to $p_{min} \approx 1.24 \times 10^{-2}$. In fact, when the uncertainties are calculated with the Birge factor $\sqrt{\chi^2/NDF}$ included, they do not vary much with the value of p_{min}. As p_{min} is increased, the truncated database fitted shrinks and so the raw uncertainties increase. However, the factor $\sqrt{\chi^2/NDF}$ decreases as the fit quality improves (despite the decrease in *NDF*) and the two effects largely compensate. **Table 3** shows that the results of the fit are reasonably stable as the criterion for the rejection of data points is varied[2].

We see from **Table 3** that the values of $g_{\pi NN}$ are compatible; converted to the usual pseudovector coupling constant[3], our result for $p_{min} \approx 1.24 \times 10^{-2}$ is

$$\frac{f_{\pi NN}^2}{4\pi} = \left(\frac{\mu_c}{2m_p}\right)^2 \frac{g_{\pi NN}^2}{4\pi} = 0.0726(14),$$

where μ_c denotes the mass of the charged pion and m_p that of the proton. This result agrees well with the value we had obtained in our previous PSA [1].

The correlation (Hessian) matrix for the seven parameters of the ETH model is given in **Table 4**; the numbers correspond to the fit for $p_{min} \approx 1.24 \times 10^{-2}$. This matrix, together with the uncertainties given in **Table 3**,

---

[1]It must be mentioned that, in Ref. [1], the results for the different p_{min} levels had been obtained by applying cuts to the distribution of the residuals, as this distribution came out in the $p_{min} \approx 2.70 \times 10^{-3}$ solution. On the contrary, the analysis here is performed separately for the different p_{min} levels.

[2]The effects, which are seen when increasing the p_{min} value from the equivalent of a 2.5 to a 3σ effect in the normal distribution, are due to the removal of the large JORAM95 π^+p data set at 44.60 MeV in the analysis of the data using the *K*-matrix parameterisations of Section 3.1. A third data point from this data set (the measurement at 14.26°) must be excluded at the last step of the iteration, thus resulting in the removal of the entire data set; were this data set not excluded, there would have been almost no change in the parameter values shown in **Table 3**.

[3]Some authors redefine $f_{\pi NN}^2$, absorbing in it the factor 4π.

enables the determination of predictions (and of their associated uncertainties) for the threshold constants, for the hadronic phase shifts and amplitudes, and for the observables at any combination of the energy and of the scattering angle. **Table 3** shows that the value of K_σ is consistent with 0; the quality of the fit would deteriorate very little if this parameter were set to 0. The value of G_σ is very little correlated with the values of the other five parameters. However, these parameters (G_ρ, K_ρ, $g_{\pi NN}$, $g_{\pi N\Delta}$, and *Z*) are all strongly correlated with each other. (As expected, the correlations among the model parameters are smaller when no floating of data sets is allowed in the fit.)

Our results for the seven model parameters have shown remarkable stability over the years, from the period when the fits were performed to old, outdated phase shifts (e.g., those of Refs. [39]) to the present times when the low-energy πN measurements are directly fitted to. The database itself has changed significantly over the past twenty or so years, with the important contributions from experiments performed at the meson factories by different research groups, which made use of different apparatuses and techniques in their experiments. Our method of applying the em corrections has also changed. Finally, various approaches have been implemented in the optimisation (e.g., in the choice of the minimisation function, from "standard" χ^2 functions [36], to robust statistics without any rejection of data [8], to the use of the Arndt-Roper formula [9] along with pruning the πN databases [1]). The observed stability is indicative of the robustness one obtains in the results when involving the ETH model in the analysis of the low-energy πN data.

3.4.2. Threshold Constants

From the parameters of the ETH model and their uncertainties given in **Table 3** for $p_{min} \approx 1.24 \times 10^{-2}$, as well as the correlation matrix given in **Table 4**, we determined the isoscalar and isovector *s*-wave scattering lengths and the isoscalar(isovector)-scalar(vector) *p*-wave scattering volumes. The results are:

$$\frac{1}{3}\tilde{a}_{0+}^{1/2} + \frac{2}{3}\tilde{a}_{0+}^{3/2} = 0.0033(12)\,\mu_c^{-1},$$

$$-\frac{1}{3}\tilde{a}_{0+}^{1/2} + \frac{1}{3}\tilde{a}_{0+}^{3/2} = -0.07698(60)\,\mu_c^{-1},$$

$$\frac{1}{3}\tilde{a}_{1-}^{1/2} + \frac{2}{3}\tilde{a}_{1-}^{3/2} + \frac{2}{3}\tilde{a}_{1+}^{1/2} + \frac{4}{3}\tilde{a}_{1+}^{3/2} = 0.2039(19)\,\mu_c^{-3},$$

$$-\frac{1}{3}\tilde{a}_{1-}^{1/2} + \frac{1}{3}\tilde{a}_{1-}^{3/2} - \frac{2}{3}\tilde{a}_{1+}^{1/2} + \frac{2}{3}\tilde{a}_{1+}^{3/2} = 0.1728(18)\,\mu_c^{-3},$$

(12)

$$\frac{1}{3}\tilde{a}_{1-}^{1/2} + \frac{2}{3}\tilde{a}_{1-}^{3/2} - \frac{1}{3}\tilde{a}_{1+}^{1/2} - \frac{2}{3}\tilde{a}_{1+}^{3/2} = -0.1830(19)\,\mu_c^{-3},$$

$$-\frac{1}{3}\tilde{a}_{1-}^{1/2} + \frac{1}{3}\tilde{a}_{1-}^{3/2} + \frac{1}{3}\tilde{a}_{1+}^{1/2} - \frac{1}{3}\tilde{a}_{1+}^{3/2} = -0.06724(83)\,\mu_c^{-3}.$$

Table 3. The values of the seven parameters of the ETH model obtained from the common fits to the truncated combined $\pi^\pm p$ elastic-scattering databases for three values of p_{min} (the confidence level in the statistical tests); these three p_{min} values correspond to a 3, 2.5, and 2σ effect in the normal distribution, respectively. The uncertainties correspond to the fit for $p_{min} \approx 1.24 \times 10^{-2}$.

	$p_{min} \approx 2.70 \times 10^{-3}$	$p_{min} \approx 1.24 \times 10^{-2}$	$p_{min} \approx 4.55 \times 10^{-2}$	uncertainty
G_σ (GeV^{-2})	27.43	27.48	27.37	0.86
K_σ	0.014	0.016	0.075	0.034
G_ρ (GeV^{-2})	54.71	54.67	55.98	0.61
K_ρ	0.66	0.66	1.35	0.41
$g_{\pi NN}$	12.84	12.84	13.07	0.12
$g_{\pi N\Delta}$	29.78	29.77	29.31	0.26
Z	-0.550	-0.552	-0.439	0.056

Table 4. The correlation matrix for the seven parameters of the ETH model for the common fit to the truncated combined $\pi^\pm p$ elastic-scattering databases for $p_{min} \approx 1.24 \times 10^{-2}$.

	G_σ	K_σ	G_ρ	K_ρ	$g_{\pi NN}$	$g_{\pi N\Delta}$	Z
G_σ	1.0000	0.5095	-0.0886	-0.0378	0.1030	-0.1602	-0.1999
K_σ	0.5095	1.0000	0.7314	0.7974	0.8847	-0.9210	0.7176
G_ρ	-0.0886	0.7314	1.0000	0.9044	0.9038	-0.8487	0.8977
K_ρ	-0.0378	0.7974	0.9044	1.0000	0.9522	-0.9284	0.9530
$g_{\pi NN}$	0.1030	0.8847	0.9038	0.9522	1.0000	-0.9497	0.9216
$g_{\pi N\Delta}$	-0.1602	-0.9210	-0.8487	-0.9284	-0.9497	1.0000	-0.9001
Z	-0.1999	0.7176	0.8977	0.9530	0.9216	-0.9001	1.0000

Converting these results to the familiar spin-isospin quantities, we obtain

$$\tilde{a}_{0+}^{3/2} = -0.0737(16)\,\mu_c^{-1}, \quad \tilde{a}_{0+}^{1/2} = 0.1573(13)\,\mu_c^{-1},$$
$$\tilde{a}_{1+}^{3/2} = 0.2090(20)\,\mu_c^{-3}, \quad \tilde{a}_{1+}^{1/2} = -0.03110(66)\,\mu_c^{-3}, \quad (13)$$
$$\tilde{a}_{1-}^{3/2} = -0.04124(78)\,\mu_c^{-3}, \quad \tilde{a}_{1-}^{1/2} = -0.0796(16)\,\mu_c^{-3}.$$

Our results for the s-wave scattering lengths $\tilde{a}_{0+}^{3/2}$ and $\tilde{a}_{0+}^{1/2}$ in Equations (13) are compatible with those obtained in Refs. [1,8,36]; these values have been very stable over the last fifteen years. The large quantity of the elastic-scattering data below 100 MeV obtained at pion factories since 1980, when analysed without influences from the data obtained at higher energies, leads to results for the s-wave scattering lengths (and hadronic phase shifts) which are significantly different from those extracted via dispersion relations after also including the $\pi^- p$ charge-exchange database in the analysis and using the measurements up to the few-GeV region.

From the results in Equations (13), we obtain

$$\tilde{a}^{cc} = \frac{2}{3}\tilde{a}_{0+}^{1/2} + \frac{1}{3}\tilde{a}_{0+}^{3/2} = 0.0803(11)\,\mu_c^{-1},$$

in good agreement with the value extracted in Ref. [1]. We have already discussed [1,33] the general disagree-ment (which, at present, is equivalent to a 4.6σ effect in the normal distribution) of our $\tilde{a}^{cc}$ value, extracted from $\pi^\pm p$ elastic-scattering measurements, with the result obtained in the pionic-hydrogen experiments at the Paul Scherrer Institut (PSI) [32], after the corrections of Ref. [33] are applied. We comment further on this issue in Section 6.1 of Ref. [4].
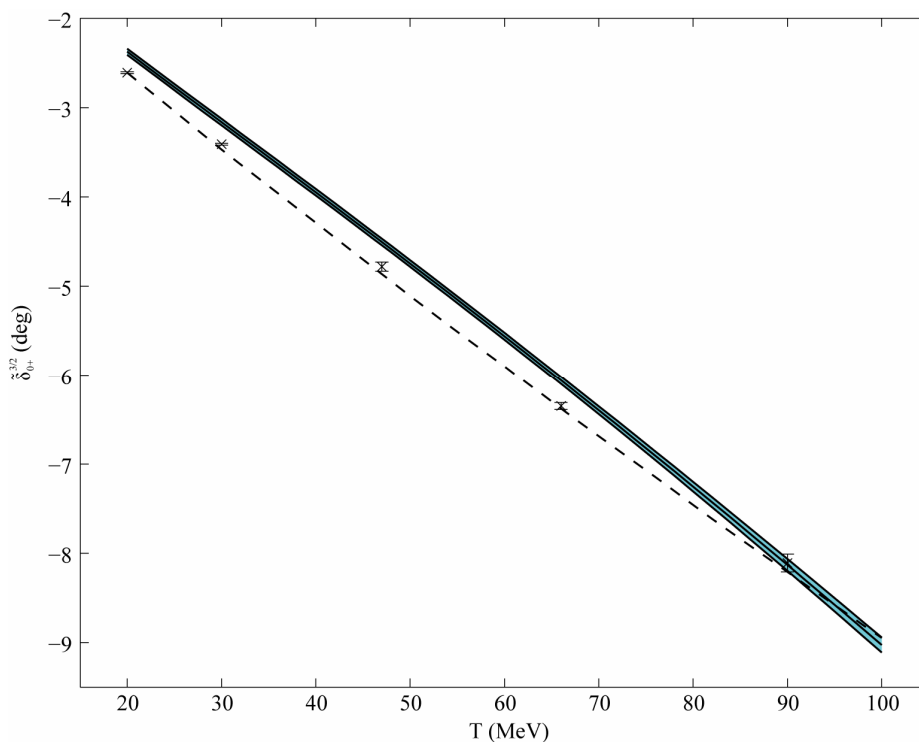
3.4.3. Hadronic Phase Shifts

The s- and p-wave hadronic phase shifts, obtained from the common fit to the truncated DB$_{+/-}$ using the ETH model, are given in **Table 5**. These phase shifts are also shown in **Figures 1-6**, together with the current SAID solution (WI08) [34] and their five single-energy values (whenever available).

It is evident from **Figures 1** and **2** that our values of the s-wave hadronic phase shifts $\tilde{\delta}_{0+}^{3/2}$ and $\tilde{\delta}_{0+}^{1/2}$ differ significantly from the SAID results. Our values of $\tilde{\delta}_{0+}^{3/2}$ are less negative, but converge towards the SAID values as the energy approaches 100 MeV; for $\tilde{\delta}_{0+}^{1/2}$, our values are consistently smaller.

For the p-wave hadronic phase shifts $\tilde{\delta}_{1+}^{3/2}$, $\tilde{\delta}_{1-}^{3/2}$, and $\tilde{\delta}_{1+}^{1/2}$, inspection of **Figures 3-5** shows that there is general agreement between the two solutions (the differences do not exceed about 0.1°). The significant difference in

Table 5. The values of the six s- and p-wave em-modified hadronic phase shifts (in degrees), obtained on the basis of the results of Tables 3 (for $p_{min} \approx 1.24 \times 10^{-2}$) and 4.

T (MeV)	$\tilde{\delta}_{0+}^{3/2}$ (S31)	$\tilde{\delta}_{0+}^{1/2}$ (S11)	$\tilde{\delta}_{1+}^{3/2}$ (P33)	$\tilde{\delta}_{1-}^{3/2}$ (P31)	$\tilde{\delta}_{1+}^{1/2}$ (P13)	$\tilde{\delta}_{1-}^{1/2}$ (P11)
20	−2.375 (34)	4.189 (27)	1.2787 (94)	−0.2239 (45)	−0.1588 (37)	−0.3687 (80)
25	−2.772 (36)	4.673 (29)	1.817 (12)	−0.3083 (63)	−0.2153 (52)	−0.486 (11)
30	−3.164 (37)	5.105 (30)	2.431 (15)	−0.3996 (83)	−0.2747 (68)	−0.602 (14)
35	−3.555 (37)	5.496 (31)	3.122 (18)	−0.497 (11)	−0.3361 (86)	−0.714 (17)
40	−3.949 (37)	5.852 (33)	3.892 (21)	−0.599 (13)	−0.399 (11)	−0.820 (20)
45	−4.345 (37)	6.180 (34)	4.744 (23)	−0.706 (16)	−0.463 (13)	−0.918 (23)
50	−4.746 (37)	6.482 (37)	5.683 (24)	−0.816 (18)	−0.527 (15)	−1.006 (27)
55	−5.151 (38)	6.760 (39)	6.715 (26)	−0.931 (21)	−0.591 (17)	−1.084 (30)
60	−5.561 (39)	7.018 (42)	7.845 (27)	−1.049 (25)	−0.655 (20)	−1.150 (34)
65	−5.977 (41)	7.256 (46)	9.081 (29)	−1.169 (28)	−0.719 (23)	−1.204 (38)
70	−6.397 (44)	7.476 (51)	10.433 (31)	−1.293 (32)	−0.782 (26)	−1.244 (42)
75	−6.823 (48)	7.679 (56)	11.909 (35)	−1.419 (36)	−0.844 (29)	−1.271 (46)
80	−7.254 (53)	7.865 (61)	13.519 (40)	−1.547 (41)	−0.906 (32)	−1.283 (50)
85	−7.690 (59)	8.036 (67)	15.277 (48)	−1.678 (45)	−0.966 (36)	−1.281 (55)
90	−8.131 (67)	8.192 (74)	17.193 (59)	−1.811 (50)	−1.026 (39)	−1.263 (60)
95	−8.577 (75)	8.334 (81)	19.282 (73)	−1.946 (55)	−1.084 (43)	−1.229 (66)
100	−9.028 (85)	8.462 (89)	21.556 (90)	−2.083 (61)	−1.141 (48)	−1.178 (71)

Figure 1. The em-modified hadronic phase shift $\tilde{\delta}_{0+}^{3/2}$ (S31) from the present work (solid curve); the band around our solution indicates 1σ uncertainties. Shown also is the current SAID solution (WI08) [34] (dashed curve), along with their five single-energy values (at T = 20, 30, 47, 66, and 90 MeV).
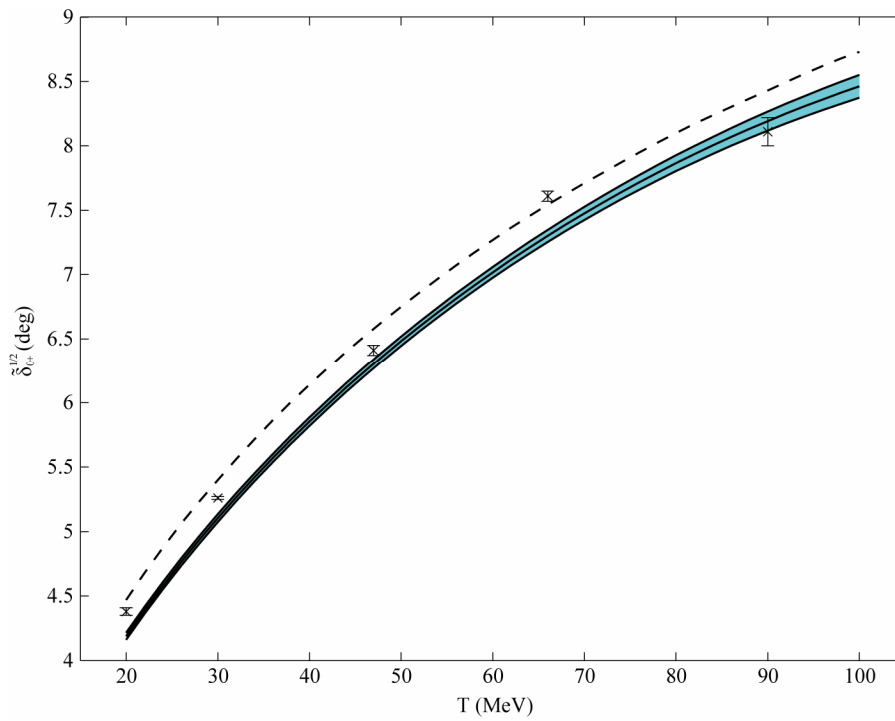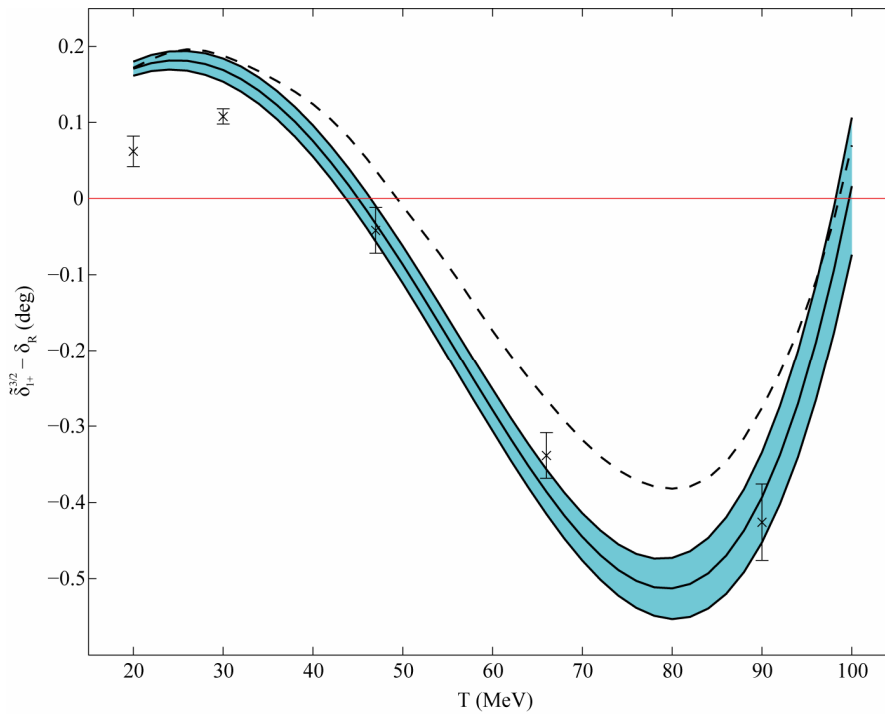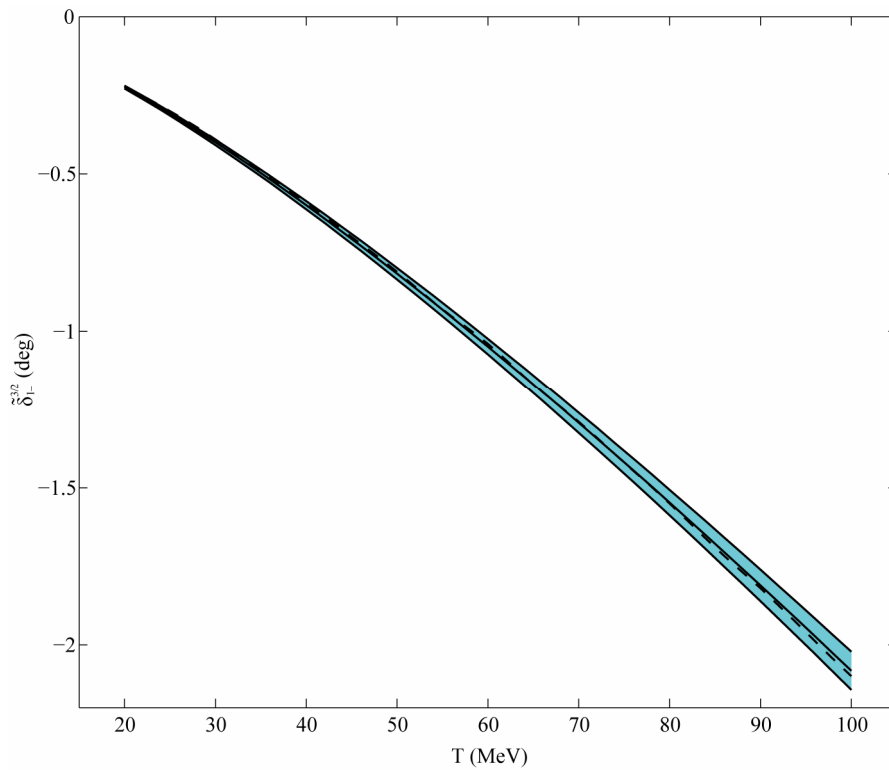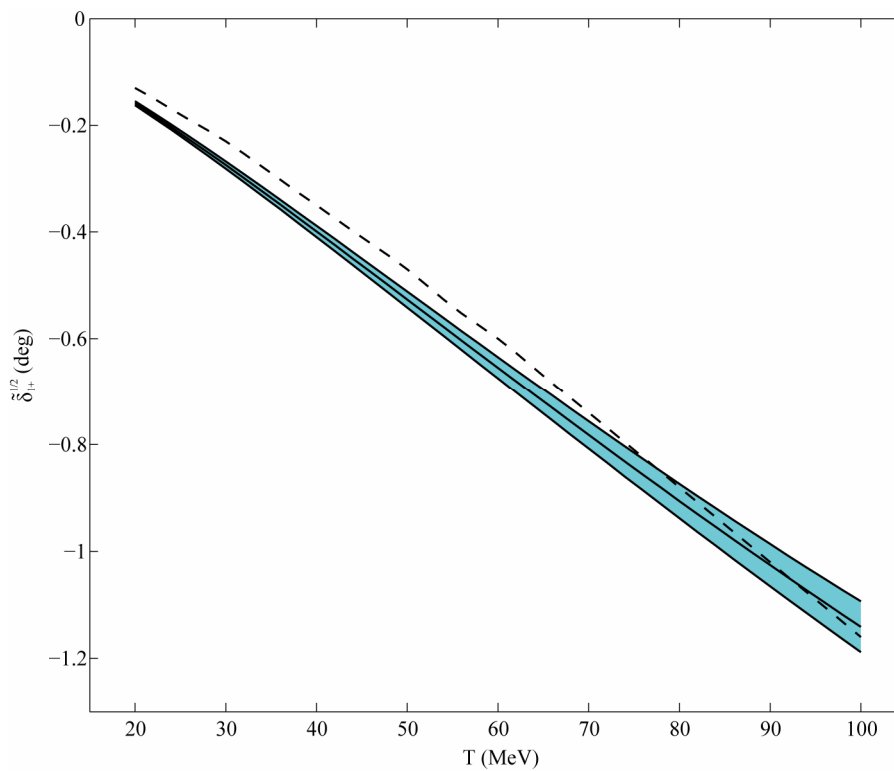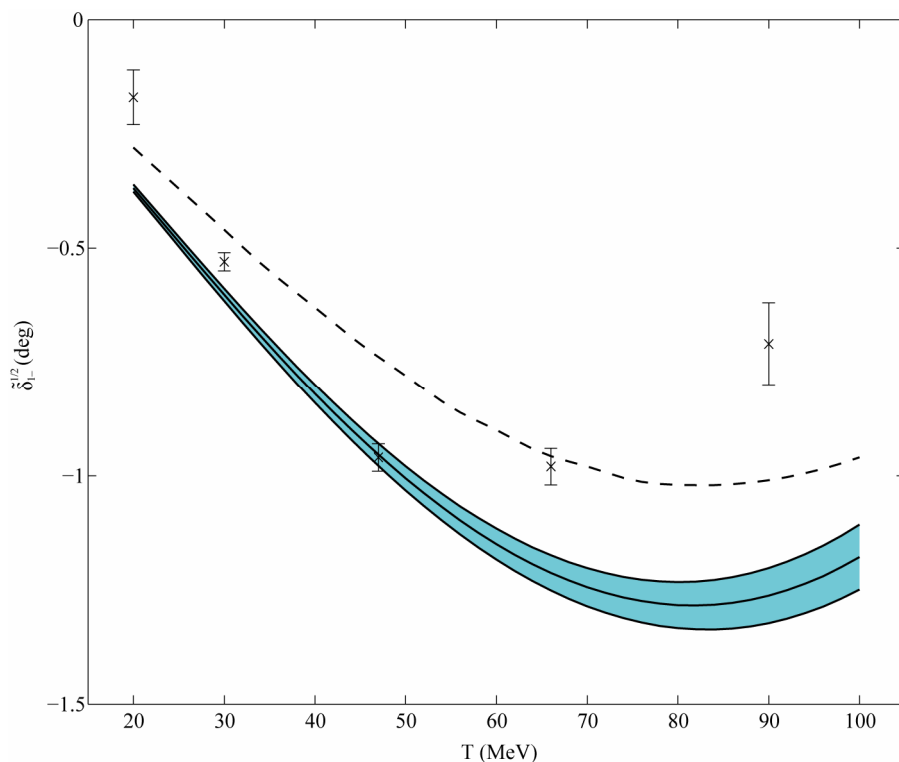
Figure 2. The em-modified hadronic phase shift $\tilde{\delta}_{0+}^{1/2}$ (S11) from the present work (solid curve); the band around our solution indicates 1σ uncertainties. Shown also is the current SAID solution (WI08) [34] (dashed curve), along with their five single-energy values (at T = 20, 30, 47, 66, and 90 MeV).

Figure 3. The em-modified hadronic phase shift $\tilde{\delta}_{1+}^{3/2}$ (P33) from the present work (solid curve); the band around our solution indicates 1σ uncertainties. Shown also is the current SAID solution (WI08) [34] (dashed curve), along with their five single-energy values (at T = 20, 30, 47, 66, and 90 MeV). To enable the meaningful comparison of the values contained in this figure, an energy-dependent baseline δ_R (= $(0.20 \times T + 1.54)$ $T \times 10^{-2}$, with T in MeV and δ_R (T) in degrees) was subtracted from all data.

Figure 4. The em-modified hadronic phase shift $\tilde{\delta}_{1-}^{3/2}$ **(P31) from the present work (solid curve); the band around our solution indicates 1σ uncertainties. Shown also is the current SAID solution (WI08) [34] (dashed curve).**

Figure 5. The em-modified hadronic phase shift $\tilde{\delta}_{1+}^{1/2}$ **(P13) from the present work (solid curve); the band around our solution indicates 1σ uncertainties. Shown also is the current SAID solution (WI08) [34] (dashed curve).**

Figure 6. The em-modified hadronic phase shift $\tilde{\delta}_{1-}^{1/2}$ (P11) from the present work (solid curve); the band around our solution indicates 1σ uncertainties. Shown also is the current SAID solution (WI08) [34] (dashed curve), along with their five single-energy values (at T = 20, 30, 47, 66, and 90 MeV).

the p-wave part of the interaction occurs for $\tilde{\delta}_{1-}^{1/2}$; our values are more negative. The values of $\tilde{\delta}_{1-}^{1/2}$, obtained in UZH06 and ZUAS12, are slightly different. This change is almost entirely due to the current use of a lower Γ_N value; at the time when the UZH06 PSA was carried out, the Particle-Data Group recommended the Γ_N value of 227.5 MeV.

Our phase-shift values are expected to be of interest in analyses involving the low-energy πN interaction, as well as in the determination of the πN σ term (e.g., see Ref. [40]).

We will now express our criticism concerning the SAID results at low energies.

- One has the impression that new πN measurements enter the SAID database without regard of whether they comprise a self-consistent set and/or of whether they are at least marginally-compatible with the data which are already part of their database. Such a strategy could be less problematic, if they had implemented robust statistics in their data analysis; instead, their results are obtained with a "standard" χ^2 function (*i.e.*, the Arndt-Roper formula), and are thus expected to be sensitive to the presence of outliers in the database (in particular, to the presence of *one-sided* outliers).
- The SAID results at low energies are literally swamp-

ed by the measurements at higher energies. In case that the floating of the data sets is allowed (as is when using the Arndt-Roper formula in the optimisation), it is unavoidable that the low-energy behaviour of the πN amplitudes will be influenced from higher energies. As a result, the low-energy experiments will be scaled systematically in such a way as to match the trends of the amplitudes suitable for the higher-energy data.

- We have not found a published plot from the SAID group, showing the energy dependence of their scale factors below 100 MeV.
- The distribution of the normalised residuals and the function which is used in the optimisation are intimately connected. In case that a χ^2 minimisation function is used, the distribution of the normalised residuals must, in a self-consistent analysis, be a Gaussian centred at 0. Any effects observed in the distribution of the normalised residuals (e.g., significant offset, asymmetry of the distribution) are indicative of problems during the fitting procedure. We have not found this information in the SAID reports or in their web site.
- By forcing the data from all three reactions into an isospin-invariant analysis scheme, SAID cannot explore a possible violation of the isospin invariance in

the hadronic part of the πN interaction.

3.4.4. Scale Factors and Normalised Residuals

We will now comment on the distribution of the scale factors z_j obtained from the common fits using the ETH model. In a "healthy" fit made on the basis of the Arndt-Roper formula, the data sets which must be scaled "upwards" should (more or less) be balanced by those which must be scaled "downwards". Additionally, the energy dependence of the scale factors over the energy range of the analysis should not be significant. If these prerequisites are not fulfilled, the parametric forms used in the fits cannot adequately reproduce the data over the entire energy range. For both the $\pi^+ p$ (**Figure 7**) and $\pi^- p$ (**Figure 8**) elastic-scattering data sets, the values of z_j which lie above and below 1 roughly balance each other and there is no discernible energy dependence[4]. Evidently, there is no subrange of the entire 30 to 100 MeV energy interval in which the data is better or worse fitted than for the rest of the range.

A second issue which must be investigated in a fit involving the minimisation of any χ^2 function is whether the distribution of the normalised residuals r_{ij}, defined as

$$r_{ij} = \frac{z_j y_{ij}^{th} - y_{ij}^{\exp}}{\delta y_{ij}^{\exp}}$$

(see Equation (1)), evaluated on the basis of the optimal parameter values, is Gaussian[5]. In practice, one fits a Gaussian function to the distribution of the normalised residuals, *i.e.*,

$$f(r) = A e^{-B(r-\bar{r})^2},$$

and investigates the quality of the fit (expressed through the corresponding χ^2 value and the NDF in the fit), as well as the asymmetry of the fitted distribution (e.g., expressed through the deviation of the extracted value of $\bar{r}$ from 0). The distribution of the normalised residuals is shown in **Figure 9**, along with the optimal Gaussian function. The χ^2 value of this fit was 33.2 for 22 DOF in the fit, whereas $\bar{r} = (1.9 \pm 4.7) \times 10^{-2}$, *i.e.*, compatible with 0. For the sake of completeness, we also give the optimal value and the uncertainty of the parameter B: $B = 0.544 \pm 0.038$; the expectation value for B is 0.5.

3.4.5. Reproduction of the MEIER04 Measurements

We will now discuss the MEIER04 measurements (which have not been included in our fits). We have created

Monte-Carlo predictions for the AP corresponding to each of their 28 data points. For the three experimental data sets, the resulting values of $\chi^2_{\min}$ were 12.5, 7.0, and 16.1, for 12, 6, and 10 DOF, respectively. The values of the scale factor for the three data sets (in the same order) are 1.011, 0.973, and 1.039; the reported normalisation uncertainty of the data is 3.5%. It is evident that our hadronic phase shifts reproduce the MEIER04 measurements very well; even the smallest p-value does not fall below 9.6×10^{-2}. This is a good test of the consistency of our approach in describing the energy and angular dependence of the $\pi^\pm p$ elastic-scattering data.

3.4.6. Reproduction of the BERTIN76 Measurements

We will now comment on the reproduction of the old measurements of Ref. [29], which are "traditionally" considered outliers in almost all modern PSAs. Reported in Ref. [29] were $\pi^+ p$ DCS measurements obtained in a broad angular interval, at seven beam energies (20.80, 30.50, 39.50, 51.50, 67.40, 81.70, and 95.90 MeV). The experimental group did not report any normalisation uncertainties for their measurements; it cannot be excluded that, at those times, the absolute normalisation was not seriously investigated in the πN experiments.

We assigned rough normalisation uncertainties to the BERTIN76 data, on the basis of the values obtained from the modern low-energy experiments which properly reported this quantity, and analysed these measurements as if they comprised the entire DB$_+$ at low energies. The analysis in terms of our general *K*-matrix parameterisations of Section 3.1 revealed that the data set at 67.40 MeV had to be eliminated due to its (very bad) shape. We were able to fit the remaining data successfully, and obtained the final χ^2 value of 55.0 for 53 DOF in the fit.

We subsequently investigated how well the phase-shift solution of the present study reproduces the BERTIN76 data; it failed. The basic problem with the BERTIN76 measurements lies with their absolute normalisation, not with their shape (though the shapes of the data sets at 39.50 and at 95.90 MeV do not pass our $p_{\min}$ criterion). For instance, for the data set at 20.80 MeV, $\hat{z}_j = 1.349$ when the overall uncertainty $\Delta \hat{z}_j$ (defined at the end of Section 2.2) is equal to 0.081; this is the most striking discrepancy in the data. The extracted $\hat{z}_j$ factors decrease almost linearly with T, reaching $\hat{z}_j = 1.027$ at 95.90 MeV. In view of these large energy-dependent effects in their absolute normalisation, we will continue excluding the BERTIN76 data in our PSAs.

4. Discussion

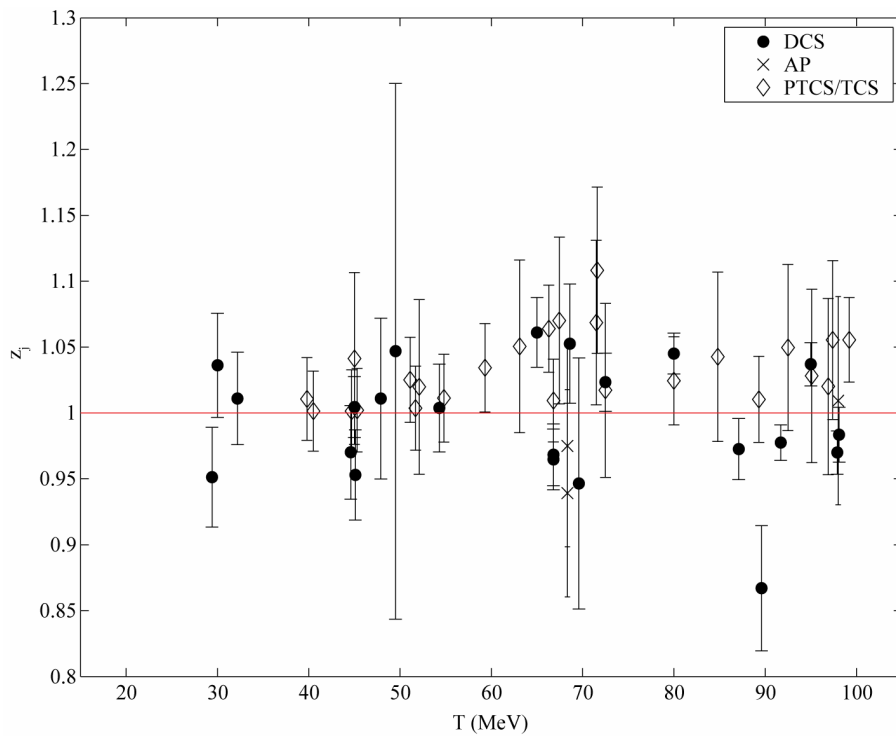In the present work, comprising the first of three papers

---

[4]The linear fit to the scale factors for the π^+p reaction yields the intercept of 1.012 ± 0.018 and the slope of $(-0.9 \pm 2.4) \times 10^{-4}$ MeV^{-1}; the linear fit to the scale factors for the $\pi^- p$ elastic-scattering reaction yields the intercept of 1.031 ± 0.018 and the slope of $(-4.5 \pm 2.4) \times 10^{-4}$ MeV^{-1}.

[5]Of course, the values of $(z_j - 1)/\delta z_j$, appearing in the second term on the rhs of Equation (1), must also be included in the distribution of the normalised residuals.

Figure 7. The scale factors z_j for the $\pi^+ p$ data, obtained from the common fit to the truncated combined $\pi^\pm p$ elastic-scattering databases using the ETH model (see Section 3.4). The values, corresponding to the two data sets which were freely floated (see Table 1), have not been included; in the case of free floating, $\left(\chi_j^2\right)_{sc} = 0$.
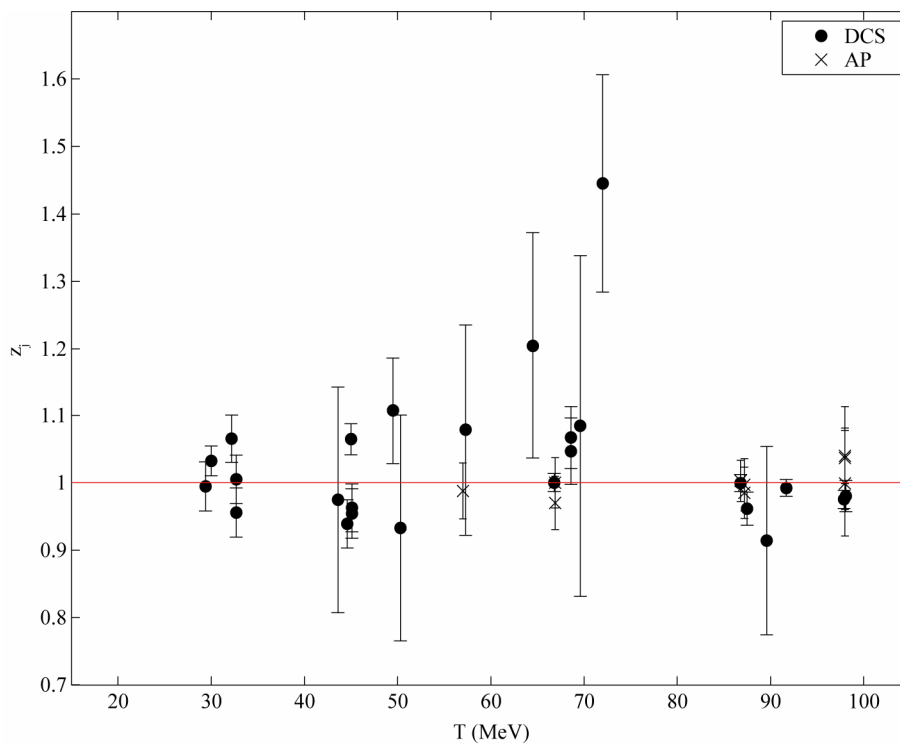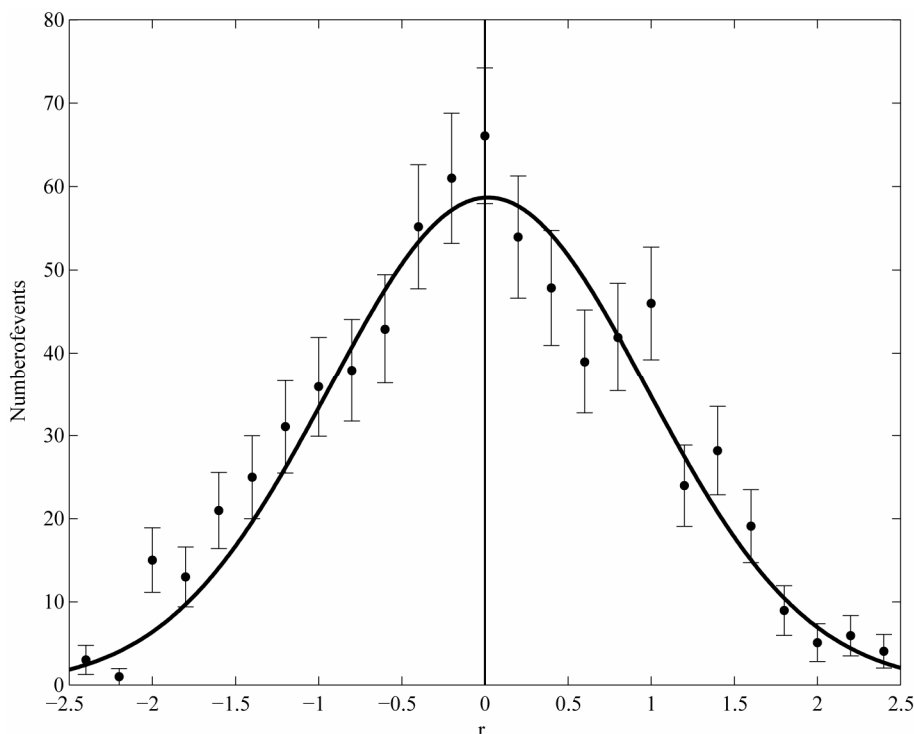

Figure 8. The scale factors z_j for the $\pi^- p$ elastic-scattering data, obtained from the common fit to the truncated combined $\pi^\pm p$ elastic-scattering databases using the ETH model (see Section 3.4). The value, corresponding to the data set which was freely floated (see Table 2), has not been included; in the case of free floating, $\left(\chi_j^2\right)_{sc} = 0$.

Figure 9. The distribution of the normalised residuals, obtained from the common fit to the truncated combined $\pi^{\pm}p$ elastic-scattering databases using the ETH model (see Section 3.4). Also shown (solid curve) is the optimal Gaussian fit to the data.

dealing with issues of the pion-nucleon (πN) interaction below pion laboratory kinetic energy of 100 MeV, we report the results of a new phase-shift analysis (PSA) of the $\pi^{\pm}p$ elastic-scattering data, using the electromagnetic (em) corrections of Refs. [5].

There are two main differences to the approach we set forth in our previous PSA [1], both pertaining to the method for the exclusion of outliers, single data points and entire data sets, in the optimisation phase. We now perform only *one* test for each data set on the only relevant quantity, namely on its contribution $\left(\chi_j^2\right)_{min}$ to the overall χ^2. In Ref. [1], we instead performed several tests (on shape, normalisation, etc.) for each data set; the use of only one test led to the exclusion of fewer data compared to Ref. [1]. The second difference concerns the imposition of a more stringent acceptance criterion of the null hypothesis in the statistical tests. Herein, we raised the minimal p-value (p_{min}) for the acceptance of the null hypothesis from the equivalent of a 3 to a 2.5σ effect in the normal distribution; the latter value is closer to the "common" choice (of most statisticians) as the outset of statistical significance.

Similarly to Ref. [1], we first investigated the self-consistency of the low-energy $\pi^{\pm}p$ elastic-scattering databases, via two separate analyses carried out (first) on the π^+p and (subsequently) on the π^-p elastic-scattering data using simple K-matrix parameterisations. We

found that it is possible to obtain self-consistent databases by removing the measurements of two π^+p and one π^-p data sets, as well as a few single data points; the removal of these outliers resulted in enormous reductions in the minimal χ^2 values for the separate fits to the two elastic-scattering databases using the K-matrix parameterisations. We give all the details concerning the accepted data sets in **Tables 1** and **2**; these details may be useful in other analyses. The aforementioned results were obtained without imposing any theoretical constraints, save for the expected low-energy behaviour of the s- and p-wave K-matrix elements and the Breit-Wigner form (see Equations (9) and (10)) for the contributions of the resonant terms.

The ETH model of Ref. [38], based on s- and u-channel diagrams with N and Δ in the intermediate states, and σ and ρ t-channel exchanges, was subsequently fitted to the truncated combined $\pi^{\pm}p$ elastic-scattering databases. The model-parameter values showed reasonable stability when subjected to different criteria for the removal of data (see **Table 3**). Our result for the pseudovector πNN coupling constant is 0.0726 ± 0.0014. On the basis of the results of the model fits, we obtained the em-modified hadronic scattering lengths and volumes (see Section 3.4.2), as well as the s- and p-wave em-modified hadronic phase shifts up to $T = 100$ MeV (see **Table 5** and **Figures 1-6**). Large differences in the s-wave part of the interaction were found when compar-

ing our hadronic phase shifts with the current SAID solution (WI08) [34] (see **Figures 1** and **2**); there is general agreement in the p waves, save for the em-modified hadronic phase shift $\tilde{\delta}_{1-}^{1/2}$.

Apart from analysing our results in terms of the assumed confidence level in the statistical tests, we also investigated the possibility of a bias in the analysis. To this end, we examined the energy dependence of the scale factors z_j, shown in **Figures 7** (for the $\pi^+ p$ data) and **8** (for the $\pi^- p$ elastic-scattering data), as well as the characteristics of the distribution of the normalised residuals (**Figure 9**). We did not find any significant deviation for these quantities from the expectations in a successful optimisation.

REFERENCES

[1] E. Matsinos, W. S. Woolcock, G. C. Oades, G. Rasche and A. Gashi, "Phase-Shift Analysis of Low-Energy $\pi^\pm p$ Elastic-Scattering Data," *Nuclear Physics A*, Vol. 778, No. 1-2, 2006, pp. 95-123. doi:10.1016/j.nuclphysa.2006.07.040

[2] E. Matsinos and G. Rasche, "Analysis of the Low-Energy $\pi^\pm p$ Elastic-Scattering Data of the CHAOS Collaboration," 2012. http://arxiv.org/abs/1203.3635

[3] H. Denz, *et al.*, "$\pi^\pm p$ Differential Cross Sections at Low Energies," *Physics Letters B*, Vol. 633, No. 2-3, 2006, pp. 209-213. doi:10.1016/j.physletb.2005.12.017

[4] E. Matsinos and G. Rasche, "Analysis of the Low-Energy $\pi^- p$ Charge-Exchange Data," 2012. http://arxiv.org/abs/1203.3856

[5] A. Gashi, E. Matsinos, G. C. Oades, G. Rasche and W. S. Woolcock, "Electromagnetic Corrections to the Hadronic Phase Shifts in Low Energy $\pi^+ p$ Elastic Scattering," *Nuclear Physics A*, Vol. 686, No. 1-4, 2001, pp. 447-462. doi:10.1016/S0375-9474(00)00603-5; A. Gashi, E. Matsinos, G. C. Oades, G. Rasche and W. S. Woolcock, "Electromagnetic Corrections for the Analysis of Low Energy $\pi^- p$ Scattering Data," *Nuclear Physics A*, Vol. 686, No. 1-4, 2001, pp. 463-477. doi:10.1016/S0375-9474(00)00604-7

[6] K. Nakamura, *et al.* (Particle Data Group), "Review of Particle Physics," *Journal of Physics G*, Vol. 37, No. 7A, 2010, Article ID: 075021. doi:10.1088/0954-3899/37/7A/075021

[7] W. R. Gibbs, Li Ai and W. B. Kaufmann, "Isospin Breaking in Low-Energy Pion-Nucleon Scattering," *Physical Review Letters*, Vol. 74, No. 19, 1995, pp. 3740-3743. doi:10.1103/PhysRevLett.74.3740

[8] E. Matsinos, "Isospin Violation in the πN System at Low Energies," *Physical Review C*, Vol. 56, No. 6, 1997, pp. 3014-3025. doi:10.1103/PhysRevC.56.3014

[9] R. A. Arndt and L. D. Roper, "The Use of Partial-Wave Representations in the Planning of Scattering Measurements. Application to 330 MeV np Scattering," *Nuclear Physics B*, Vol. 50, No. 1, 1972, pp. 285-300. doi:10.1016/S0550-3213(72)80019-1

[10] E.G. Auld, *et al.*, "$\pi^+ - p$ Elastic Scattering at 47.9 MeV," *Canadian Journal of Physics*, Vol. 57, No. 1, 1979, pp. 73-78. doi:10.1139/p79-008

[11] B. G. Ritchie, *et al.*, "$\pi^+ p$ Scattering at 65 to 140 MeV," *Physics Letters B*, Vol. 125, No. 2-3, 1983, pp. 128-132. doi:10.1016/0370-2693(83)91251-0

[12] J. S. Frank, *et al.*, "Measurement of Low-Energy Elastic $\pi^\pm p$ Differential Cross Sections," *Physical Review D*, Vol. 28, No. 7, 1983, pp. 1569-1585. doi:10.1103/PhysRevD.28.1569

[13] J. T. Brack, *et al.*, "πp Elastic Scattering from 67 to 139 MeV," *Physical Review C*, Vol. 34, No. 5, 1986, pp. 1771-1778. doi:10.1103/PhysRevC.34.1771

[14] J. T. Brack, *et al.*, "Large-Angle $\pi^+ p$ Elastic Scattering at 66.8 MeV," *Physical Review C*, Vol. 38, No. 5, 1988, pp. 2427-2429. doi:10.1103/PhysRevC.38.2427

[15] U. Wiedner, *et al.*, "Hidden Strangeness in the Proton? Determination of the Real Part of the Isospin-Even Forward-Scattering Amplitude of Pion-Nucleon Scattering at 54.3 MeV," *Physical Review D*, Vol. 40, No. 11, 1989, pp. 3568-3581. doi:10.1103/PhysRevD.40.3568

[16] J. T. Brack, *et al.*, "Absolute Differential Cross Sections for $\pi^\pm p$ Elastic Scattering at $30 \leq T_\pi \leq 67$ MeV," *Physical Review C*, Vol. 41, No. 5, 1990, pp. 2202-2214. doi:10.1103/PhysRevC.41.2202

[17] J. T. Brack, *et al.*, "Forward Angle $\pi^\pm p$ Elastic Scattering Differential Cross Sections at $T_\pi = 87$ to 139 MeV," *Physical Review C*, Vol. 51, No. 2, 1995, pp. 929-936. doi:10.1103/PhysRevC.51.929

[18] Ch. Joram, *et al.*, "Low-Energy Differential Cross Sections of Pion-Proton ($\pi^\pm p$) Scattering. I. The Isospin-Even Forward Scattering Amplitude at $T_\pi = 32.2$ and 44.6 MeV," *Physical Review C*, Vol. 51, 1995, pp. 2144-2158. doi:10.1103/PhysRevC.51.2144; Ch. Joram, *et al.*, "Low-Energy Differential Cross Sections of Pion-Proton ($\pi^\pm p$) Scattering. II. Phase Shifts at $T_\pi = 32.7$, 45.1, and 68.6 MeV," *Physical Review C*, Vol. 51, No. 4, 1995, pp. 2159-2165. doi:10.1103/PhysRevC.51.2159

[19] M. E. Sevior, *et al.*, "Analyzing Powers in $\pi^\pm \vec{p}$ Elastic Scattering from $T_\pi = 98$ to 263 MeV," *Physical Review C*, Vol. 40, No. 6, 1989, pp. 2780-2788. doi:10.1103/PhysRevC.40.2780

[20] R. Wieser, *et al.*, "Measurement of the $\pi^+ \vec{p}$ Analyzing Power at 68.3 MeV," *Physical Review C*, Vol. 54, No. 4, 1996, pp. 1930-1934. doi:10.1103/PhysRevC.54.1930

[21] B. J. Kriss, *et al.*, "Pion-Proton Integral Cross Section Measurements," *πN Newsletter*, Vol. 12, 1997, pp. 20-25; B. J. Kriss, *et al.*, "Pion-Proton Integral Cross Sections at $T_\pi = 40$ to 284 MeV," *Physical Review C*, Vol. 59, No. 3, 1999, pp. 1480-1487. doi:10.1103/PhysRevC.59.1480

[22] E. Friedman, "Partial Total πN Cross Sections," *πN Newsletter*, Vol. 15, 1999, pp. 37-42.

[23] A. A. Carter, J. R. Williams, D. V. Bugg, P. J. Bussey and D. R. Dance, "The Total Cross Sections for Pion-Proton Scattering between 70 MeV and 290 MeV," *Nuclear Physics B*, Vol. 26, No. 3, 1971, pp. 445-460. [doi:10.1016/0550-3213(71)90188-X](doi:10.1016/0550-3213(71)90188-X)

[24] E. Pedroni, *et al.*, "A Study of Charge Independence and Symmetry from π^+ and π^- Total Cross Sections on Hydrogen and Deuterium near the 3,3 Resonance," *Nuclear Physics A*, Vol. 300, No. 2, 1978, pp. 321-347. [doi:10.1016/0375-9474(78)96136-5](doi:10.1016/0375-9474(78)96136-5)

[25] M. Janousch, *et al.*, "Destructive Interference of *s* and *p* Waves in 180° $\pi^- p$ Elastic Scattering," *Physics Letters B*, Vol. 414, No. 3-4, 1997, pp. 237-241. [doi:10.1016/S0370-2693(97)01169-6](doi:10.1016/S0370-2693(97)01169-6)

[26] J. C. Alder, *et al.*, "Measurement of the Asymmetry Parameter A in $\pi^- p$ Elastic and Charge-Exchange Scattering at Pion Energies T_π = 98, 238, 292, and 310 MeV," *Physical Review D*, Vol. 27, No. 5, 1983, pp. 1040-1055. doi:10.1103/PhysRevD.27.1040

[27] G. J. Hofman, *et al.*, "Analyzing Powers for $\pi^\pm \bar{p}$ Elastic Scattering between 87 and 263 MeV," *Physical Review C*, Vol. 58, No. 6, 1998, pp. 3484-3493. doi:10.1103/PhysRevC.58.3484

[28] J. D. Patterson, *et al.*, "Analyzing Powers for πp Elastic Scattering between 57 and 139 MeV," *Physical Review C*, Vol. 66, No. 2, 2002, Article ID: 025207. doi:10.1103/PhysRevC.66.025207

[29] P. Y. Bertin, *et al.*, "$\pi^+ p$ Scattering below 100 MeV," *Nuclear Physics B*, Vol. 106, 1976, pp. 341-354. [doi:10.1016/0550-3213(76)90383-7](doi:10.1016/0550-3213(76)90383-7)

[30] P. J. Bussey, *et al.*, "πp Elastic Scattering from 88 to 292 MeV," *Nuclear Physics B*, Vol. 58, No. 2, 1973, pp. 363-377. [doi:10.1016/0550-3213(73)90589-0](doi:10.1016/0550-3213(73)90589-0)

[31] R. Meier, *et al.*, "Low Energy Analyzing Powers in Pion-Proton Elastic Scattering," *Physics Letters B*, Vol. 588, No. 3-4, 2004, pp. 155-162. doi:10.1016/j.physletb.2004.02.071

[32] H.-Ch. Schröder, *et al.*, "The Pion-Nucleon Scattering Lengths from Pionic Hydrogen and Deuterium," *European Physical Journal C*, Vol. 21, No. 3, 2001, pp. 473-488. [doi:10.1007/s100520100754](doi:10.1007/s100520100754)

[33] G. C. Oades, G. Rasche, W. S. Woolcock, E. Matsinos and A. Gashi, "Determination of the *s*-Wave Pion-Nucleon Threshold Scattering Parameters from the Results of Experiments on Pionic Hydrogen," *Nuclear Physics A*, Vol. 794, No. 1-2, 2007, pp. 73-86. doi:10.1016/j.nuclphysa.2007.07.007

[34] R. A. Arndt, W. J. Briscoe, I. I. Strakovsky and R. L. Workman, "Extended Partial-Wave Analysis of πN Scattering Data," *Physical Review C*, Vol. 74, No. 4, 2006, Article ID: 045205. doi:10.1103/PhysRevC.74.045205

[35] F. James, "MINUIT—Function Minimization and Error Analysis," CERN Program Library Long Writeup D506.

[36] N. Fettes and E. Matsinos, "Analysis of Recent $\pi^+ p$ Low-Energy Differential Cross-Section Measurements," *Physical Review C*, Vol. 55, No. 1, 1997, pp. 464-473. doi:10.1103/PhysRevC.55.464

[37] T. E. O. Ericson and W. Weise, "Pions and Nuclei," Clarendon Press, Oxford, 1988.

[38] P. F. A. Goudsmit, H. J. Leisi, E. Matsinos, B. L. Birbrair and A. B. Gridnev, "The Extended Tree-Level Model for the Pion-Nucleon Interaction," *Nuclear Physics A*, Vol. 575, No. 4, 1994, pp. 673-706. [doi:10.1016/0375-9474(94)90162-7](doi:10.1016/0375-9474(94)90162-7)

[39] R. Koch and E. Pietarinen, "Low-Energy πN Partial Wave Analysis," *Nuclear Physics A*, Vol. 336, No. 3, 1980, pp. 331-346. [doi:10.1016/0375-9474(80)90214-6](doi:10.1016/0375-9474(80)90214-6); R. Koch, "A Calculation of Low-Energy πN Partial Waves Based on Fixed-*t* Analyticity," *Nuclear Physics A*, Vol. 448, No. 4, 1986, pp. 707-731. [doi:10.1016/0375-9474(86)90438-0](doi:10.1016/0375-9474(86)90438-0)

[40] J. M. Alacrón, J. M. Camalich and J. A. Oller, "Chiral Representation of the πN Scattering Amplitude and the Pion-Nucleon Sigma Term," *Physical Review D*, Vol. 85, No. 5, 2012, Article ID: 051503. doi:10.1103/PhysRevD.85.051503